Ozone variations over Central Tien-Shan in Central Asia and Implications for Regional Emissions Reduction Strategies

Boris B. Chen[1], Sanjar A. Imashev[1*], Leonid G. Sverdlik[1], Paul A. Solomon[2], Jeffrey Lantz[3], James J. Schauer[4], Martin M. Shafer[4], Maria S. Artamonova[5], Greg R. Carmichael[6]

[1] *Kyrgyz-Russian Slavic University, 44 Kievskaya Str., Bishkek 720000, Kyrgyz Republic,*

[2] *U.S. Environmental Protection Agency, Office of Research & Development, Las Vegas, NV 89119 USA,*

[3] *U.S. Environmental Protection Agency, Office of Radiation and Indoor Air, Las Vegas, NV 89119 USA,*

[4] *Wisconsin State Laboratory of Hygiene, University of Wisconsin, 660 North Park St, Madison, WI 53706, USA, Environmental Chemistry and Technology Program, 660 North Park St, University of Wisconsin, Madison 53706, USA,*

[5] *Institute of Atmospheric Physics, 109017 Moscow, Russia,*

[6] *Department of Chemical & Biochemical Engineering, the University of Iowa, Iowa City, IA 52242.*

[*] Corresponding Author: Tel: 996-312-431-197; Fax: 996-312-431-171
E-mail address: sanjar_imashev@krsu.edu.kg

Abstract

The variability of total column ozone (TCO) and tropospheric column ozone (TrCO) was examined in Central Asia. Measurements were conducted at the Lidar Station Teplokluchenka in eastern Kyrgyzstan for one year, July 2008 – July 2009.

TCO was obtained using a handheld Microtops II Ozonometer (TCO-MII) and from the AURA OMI (TCO-OMI) satellite. Nitrogen dioxide (NO_2) and formaldehyde concentrations also were obtained from the OMI satellite. Formaldehyde was used as a surrogate for volatile organic compounds. TrCO was estimated by the difference between TCO-OMI and stratospheric column ozone retrieved from the MLS satellite. Comparison of the ground-based TCO-MII with TCO-OMI showed good agreement (r^2=0.93). Linear regression between the two was used to estimate missing values in the TCO-MII dataset.

The contribution of TrCO to TCO varied from 15% in summertime to 5% in winter. High values of TrCO were observed during the summer (July 45 DU) and low values during the winter (December 15 DU) as are typically observed. Average values of TrCO for summer, autumn, winter, and spring were equal to 42, 27, 20, and 30 DU, respectively. Seasonal variability of TrCO corresponded to solar intensity, indicating that TrCO was likely formed through photochemistry rather than stratospheric intrusion.

The spatial distribution of NO_2 and VOC were examined to better understand the regional sources of these ozone precursors. Transport from highly populated areas of the Ferghana Valley and Tashkent in Uzbekistan contribute to the TrCO concentrations observed. The HCHO/NO_2 ratio, an indicator of ozone production rate, suggested that reducing NO_2 would be more effective at reducing TrCO during most of the year, except summer where reductions of both would likely be needed.

Keywords: Total column ozone; Tropospheric ozone; OMI Satellite; HCHO/NO_2; NOx versus VOC limited

INTRODUCTION

Ozone plays an important role in atmospheric processes and can positively or negatively influence human health and the environment depending on its location in the atmosphere. Ozone in the stratosphere filters out harmful ultra-violet radiation from the sun, protecting life on earth. In the lower troposphere ozone is considered a dangerous pollutant negatively influencing human health and ecosystems (EPA 2006; Gurjar *et al.*, 2010), being a key constituent of urban smog. Ozone in the troposphere is the third most important greenhouse gas (Fuhrer and Booker, 2003; Forster *et al.*, 2007). While the level of tropospheric ozone in Europe and North America has decreased since the 1980's due to the reduction of precursor emissions [for example, NOx (classically defined as NO + NO_2) and volatile organic compounds (VOC)], it continues to increase in the Asian region (Jonson *et al.*, 2006). Burning of biomass, such as residential cooking and heating, which are sources of non-methane hydrocarbons and NOx, also contribute to tropospheric ozone formation especially in densely populated areas of developing countries. Previous studies connected with the measurement of NO_2 in the Tien-Shan region occurred during the ground-based validation of satellite NO_2 vertical column data (EOS-Aura OMI) in 2004-2006 (Ionov *et al.*, 2008). The satellite and ground-based data over Issyk-Kul (~120 km to the west from Lidar-Site) agreed within (~0.26 ±0.28) × 10^{15} molec/cm^2, with correlation coefficient of 0.87. Validation of tropospheric measurements by the OMI NO_2 satellite also was discussed. In particular, satellite global mapping of NO_2 tropospheric columns indicated that NO_x sources near Issyk-Kul station, such as the city of Almaty, Kazakhstan, the city of Tashkent, Uzbekistan and Urumchi, China might affect observations over Issyk-Kul (Fig. 1). In addition to constant emissions from the urban centers, tropospheric NO_2 in the region may rise episodically due to long-range transport. For example, Mei *et al.* (2011) reported significant increases in tropospheric column NO_2 over Kyrgyzstan due to smoke plumes from wildfires in Western Russia, which occurred in August 2010.

Air pollution monitoring in remote regions, such as Central Tien-Shan of Central Asia, can provide valuable information about regional emissions sources and characteristics of pollutant transport (especially long-range) necessary for validation of regional and global models as well as provide insight in to precursor emissions management strategies designed to reduce tropospheric ozone.

This study examines the variability of total column ozone (TCO) and tropospheric column ozone (TrCO) in the Central Tien-Shan region of Central Asia. The information is an important step forward in the assessment of air pollution effects and air quality in the Central Asia region, since past studies of trace gases in the region were mainly connected with the ground-based validation of satellite measurements and referred basically to total column amounts rather then tropospheric content (e.g., Ionov *et al.*, 2006, 2008). These measurements coincide with a larger study that obtained first time particulate matter mass and detailed chemical composition at two sites during the same time period in Central Asia (Miller-Schulze *et al.*, 2011).

EXPERIMENTAL

Site description

Tien-Shan is a mountain system located in Central Asia. Its name is Chinese for "Celestial Mountains." This mountain range lies to the north and west of the Taklimakan Desert, in the eastern border region of Kazakhstan, the western regions of China, and covers over 80% of Kyrgyzstan. Due to their location, the Tien-Shan Mountains play an important role in the water budget for central Asia region.

Measurements were conducted in the north-eastern part of Kyrgyzstan (N 42.47, E 78.53) at 2000 m above sea level at the Lidar Station Teplokluchenka of the Kyrgyz-Russian Slavic

University (Lidar-Site) (see Fig. 1). The site is located away from urban and industry pollution sources making it suitable for examining regional air quality and long-range pollutant transport.

Instrumentation

The study was conducted from June 2008 through May, 2009. Total column ozone (integrated ozone from the ground to the top of the atmosphere) was measured by a Microtops II Ozonometer (TCO-MII, Solar Light Co). The MII is a handheld compact spectrophotometer for the simultaneous measurement of direct solar ultra-violet radiation at three discrete wavelengths (305, 312 and 320 nm), TCO-MII in Dobson units (DU), precipitable water column (936 nm), and aerosol optical thickness (1020 nm). The ozonometer has a low noise level (about 0.0002%), a low non-linearity (less than 0.0015%), and has an accuracy of <2% for total ozone measurements based on the manufacturers specifications, which is comparable to the accuracy of more sophisticated and expensive ozone monitoring equipment (Morys *et al.*, 2001). TCO-MII measurements were obtained during clear sky conditions and midday hours at sun culmination when the air mass in the line of sight to the sun was at a minimum. This time period is also coincide with overpass time of nadir viewing Aura-OMI. Measurements made in heavy clouds condition were described by site operators using special code (ID) and were excluded from the analysis.

Total column ozone and formaldehyde (HCHO) also were obtained from the Ozone Monitoring Instrument (OMI) flying on the National Aeronautics and Space Administration's Earth Observing System Aura satellite (Levelt *et al.*, 2006; Duncan *et al.*, 2010). Open access to these data is provided by the Mirador project (http://mirador.gsfc.nasa.gov/). The TCO-OMI data had a 1 degree horizontal spatial resolution in the study region as opposed to a more localized column measurement using the MII. Temporal variations of TCO by both methods at the Lidar site location is shown in Figure 2. Tropospheric column ozone (TrCO) was obtained by subtracting

stratospheric column ozone (SCO) obtained from the Microwave Limb Sounder (MLS) satellite from TCO-OMI. These data were retrieved from the NASA Goddard Homepage For Tropospheric Ozone (http://acd-ext.gsfc.nasa.gov/Data_services/cloud_slice/) (Ziemke *et al.*, 2006). Tropospheric column NO_2 was obtained from the Giovanni system (http://gdata2.sci.gsfc.nasa.gov/daac-bin/G3/gui.cgi?instance_id=omil2g).

RESULTS AND DISCUSSION

Comparison of ground-based and satellite TCO

The temporal variation of TCO for the study period by both methods is illustrated in Fig. 2. This comparison shows excellent agreement between the two methods during the year (June 2008 to May 2009) with an overall $r^2 = 0.931$, a slope of 0.94 (MII/OMI), and a small intercept (31 DU) (Fig. S1 in Supplemental Information). A comparison of TCO values for each month during the study period showed good agreement even on these shorter time scales with correlation coefficients (r^2) ranging from 0.81-0.98. Although the TCO-MII results are consistently higher than the TCO-OMI results, the good agreement allows the regression relationship to be used to estimate missing values in the TCO-MII dataset (79 values). This is important since clouds interfere with the TCO-MII ground-based measurement and since the MII provides a more localized columnar value rather than the 1 degree average resolution of the OMI method. A more robust dataset also is obtained using this approach.

Total column ozone

The spatial and temporal distribution of TCO-OMI in the region was typical for moderate latitudes of the northern hemisphere (Figure 2, 3), in line with Brewer-Dobson circulation (James, 1995; Shepherd, 2007).

For example, maximum values of TCO in the northern hemisphere are observed at the beginning of spring (monthly averages ranging from 345 – 355 DU) with monthly average minimum values in autumn (October 290 DU) (Seinfeld and Pandis, 2006).

Maximal and minimal single day values of TCO at the Lidar-Site were observed in March, 2009 and December, 2008 and reached 414 DU and 224 DU, respectively. These results are consistent with the long-term seasonal monthly trends as shown in Figure 4 for middle-latitude (40-45˚N). This figure shows values of TCO for the period from 1997 until 2005, retrieved from Total Ozone Mapping Spectrometer (TOMS) on the Earth Probe Satellite T (http://toms.gsfc.nasa.gov/). There is a clear autumn minimum in October and spring maximum in March.

Tropospheric column nitrogen dioxide

Ozone generation in the troposphere requires the presence of nitrogen oxides (NOx), which are emitted primarily from mobile sources, utilities, and other high temperature industrial combustion sources (Seinfeld and Pandis, 2006). NOx contributes to a variety of environmental problems: e.g., health effects (NO_2), acid rain and acidification of aquatic systems, ground level ozone (smog), and visibility degradation. Natural sources such as lightning and soil also contribute to atmospheric levels of NOx (Peirce and Aneja, 2000; Aneja, 2001).

Monthly average values of nitrogen dioxide (NO_2) in the tropospheric column (Boersma *et al.*, 2004), retrieved from the Aura OMI satellite (http://www.knmi.nl/omi/research/product/product_generator.php?info=intro&product=NO2)

covering an area from (35-46 N) latitude to (65-85 E) longitude, from June 2008 through May 2009, are illustrated in Fig. 5. Comparison of Aura OMI NO_2 vertical column data with collocated ground-based measurements showed biases over Kyrgyzstan (Ionov *et al.*, 2008), which can be due to the detection of pollution in the tropospheric by OMI, but not observed in the ground-based measurements, as the zenith sky observation in twilight was slightly sensitive to tropospheric NO_2. Comparisons with in situ and ground-based data suggest that the OMI tropospheric NO_2 columns are biased by ~5% (Lamsal *et al.*, 2010). The overall error in the vertical, tropospheric NO_2 column data is 10-40% (Boersma *et al.*, 2007). High values were observed in the warm period (1.05×10^{15} molec/cm^2 maximum in July) while low values were observed during the cold period (0.32×10^{15} molec/cm^2 minimum in November). Overall, the annual variability of TrCO and NO_2 were in good agreement with each other (r^2=0.76), suggesting that a significant fraction of the NO_2 was formed in the atmosphere as part of the same photochemical activity responsible for ozone formation (Tiwary and Colls, 2010). In contrast to the summer maximum of tropospheric NO_2 observed at the remote and mountainous Lidar-Site, a winter maximum was observed in urban areas of the region (Fig. S2 in Supplemental Information), probably due to domestic heating activities and poor pollutant dispersion due to the lower temperatures.

The annual average value of tropospheric NO_2 at Lidar-Site (0.63×10^{15} molec/cm^2) is comparable to values observed over Issyk-Kul station reported by Ionov *et al.* (2008): 0.72×10^{15} molec/cm^2 (Aura-OMI) and 1.19×10^{15} molec/cm^2 (Envisat SCIAMACHY). Higher values over Issyk-Kul station may be due to the close proximity a local pollution sources - the city of Almaty (the former capital of Kazakhstan) with annual tropospheric NO_2 of 3.96×10^{15} molec/cm^2.

In particular, regardless of the season the highest values of tropospheric NO_2 equal to about 4 to 10×10^{15} molec/cm^2 are observed in Uzbekistan (Fig. 6) – near to Andizhan, Namangan and Ferghana cities located in Ferghana Valley and near Tashkent city (see Fig. 1). The Ferghana

Valley is the most populous area in Central Asia including approximately 20% of the total population in the region with a population density of 200-500 persons per km^2. Industry in the valley includes agriculture, metallurgy, and oil production among others (UNEP, 2005). Atmospheric inversions, due to the geography of the area, result in a buildup of pollutants that can be transported to Kyrgyzstan due to so-called westerlies; prevailing winds of the middle latitudes (between about 30°and 60° in both hemispheres) that blow in the Northern Hemisphere from the Southwest direction.

Volatile organic compounds in tropospheric column

Formaldehyde can act as a proxy for volatile organic compounds (VOCs) as it is produced during the oxidation of other VOCs. Martin *et al.* (2004) used the ratio of the tropospheric columns of HCHO and NO_2 from the Global Ozone Monitoring Experiment (GOME) instrument to reflect the sensitivity of ozone formation to precursor species concentrations. The same approach was used by Duncan *et al.* (2010), except for using Aura-OMI data instead of GOME data due to finer horizontal resolution of the first instrument, which can provide additional detail on urban-rural spatial gradients. The main biogenic precursor of HCHO is isoprene, a VOC that is emitted naturally from trees. HCHO in industrial regions is produced by the oxidation of anthropogenic hydrocarbons and from bio-fuels (Seinfeld and Pandis, 2006). Overall the error in the satellite HCHO column data is estimated to be 25-31% (Millet *et al.*, 2006). The precision of Aura HCHO data product on a 1° × 1° grid is of the order 1×10^{15} molec/cm^2 (Veefkind *et al.*, 2011).

The annual average spatial distribution of HCHO over the region for the study period is shown in Fig. 7. The annual average value of total column HCHO at Lidar-Site was equal to 3.16×10^{15} molec/cm^2. HCHO values (in 10^{15} molec/cm^2) in summer, autumn, winter 2008 and spring 2009

were equal to 1.49, 5.55, 5.16, and 7.62, respectively. Seasonally averaged spatial plots of HCHO are given in Supplemental Information (Fig. S3).

The ratio of OMI HCHO to NO_2 can provide insight into emissions management strategies suggesting which pollutant might be most effective at reducing ozone levels in the area (i.e., which is the limiting reagent in the production of ozone through the NOx + VOC $\leftrightarrow$ O_3 reaction, where the HCHO/NO_2 provides information on the sensitivity of the production of ozone but not concentration, as other factors can impact concentration). For example, if the HCHO/NO_2 ratio is low (<1) then reducing anthropogenic VOC would be most effective (VOC is the limiting reagent) (Duncan *et al*., 2010; Kumar *et al.*, 2008). On the other hand, if the HCHO/NO_2 is high (>2) then reducing NOx would be most efficient. In the transition between a ratio of 1 and 2 reducing both HCHO and NO_2 would likely be needed.

Seasonal HCHO to NO_2 ratios were equal to 1.75, 10.68, 10.61, and 12.04 for summer, autumn, winter 2008 and spring 2009, respectively. The annual ratio of HCHO to NO_2 was equal to 5. In these cases, the better strategy to reduce surface ozone is to reduce NOx (Duncan *et al.*, 2010), except during the summer when reducing of both VOC and NOx likely would be more beneficial.

Tropospheric column ozone

The majority of TrCO generation occurs when nitrogen oxides, carbon monoxide, and VOC react in the atmosphere in the presence of sunlight (Seinfeld and Pandis, 2006). The major anthropogenic sources of these ozone precursors are motor vehicle exhaust, industrial emissions, and chemical solvents as noted above. Biogenic or natural emissions also can be important.

The spatial distribution of TrCO obtained from AURA OMI/MLS satellites is shown in Fig. 8. Higher values are observed over densely populated and industrial areas of Uzbekistan and

Kazakhstan in relation to the Kyrgyzstan territory. It is also clear, that low values of TrCO are observed over under-populated rural areas (mainly mountainous regions) of Kyrgyzstan, especially in cold periods.

Temporal variations of monthly average values of TrCO at the Lidar-Site are presented in Fig. 9. High values of TrCO were observed during the summer with the monthly average maximum in July (45 DU) and low values during the winter with the minimum in December (15 DU). These values correspond to about 75 and 25 ppbv, respectively (Ziemke *et al.*, 2006). Average values of TrCO for the summer, autumn, winter and spring periods were equal to 42, 27, 20 and 30 DU, respectively. The contribution of TrCO to TCO varied from 15% in summertime up to 5% in the winter with an annual average value of 9.5% (Fig. 10).

Seasonal values correspond to solar radiation intensity, suggesting the larger contribution of photochemistry to tropospheric ozone generation in comparison with stratosphere-tropospheric exchange. These results are in agreement with others (e.g., Seinfeld and Pandis 2006; Guicherit and Roemer, 2000). As in the U.S. (EPA 2006), reduction of ozone in Kyrgyzstan may require regional reductions of NOx and VOC in industrialized and urban areas upwind and in this case outside of Kyrgyzstan. A more detailed study, including surface-based measurements at multiple locations both locally and regionally will be needed to develop effective strategies for reducing ozone in the study area.

CONCLUSIONS

This paper describes the seasonal variability of total column ozone (TCO) and tropospheric column ozone (TrCO) observed over a year period at Lidar Station Teplokluchenka (2000 m above sea level) in Central Tien-Shan. Comparison of ground-based TCO-MII with satellite TCO-OMI showed good agreement (r^2=0.93). The resulting regression equation was used to

replace missing values in MII dataset. Observed seasonal variations of TCO were typical for mid-latitudes of the northern hemisphere, with highest values at the beginning of spring and lowest values in autumn. Contribution of TrCO to TCO varied from 15% in summer up to 5% in the winter and 9.5% on the average for the year. The seasonal variation of TrCO corresponded to periods of solar radiation intensity and indicated a higher contribution of photochemistry to the formation of tropospheric ozone in comparison with stratosphere-troposphere exchange. High values of TrCO during the summer period (up to 45 DU) were result of photochemical generation connected with anthropogenic sources of nitrogen oxides and VOCs likely transported to the area from the industrial and densely populated areas of Uzbekistan - Ferghana valley and around Tashkent city. The ratio of HCHO to NO_2 indicated that reducing NO_2 would be more effective at reducing TrCO during most of the year, except summer where reductions of both NO_2 and VOC would likely be needed.

ACKNOWLEDGEMENT

The U.S. Environmental Protection Agency through its Office of Research and Development funded this study and collaborated in the research described here under Contract EP-D-06-001 to the University of Wisconsin-Madison as a component of the International Science & Technology Center (ISTC) project # 3715 (Transcontinental Transport of Air Pollution from Central Asia to the US) funded by the EPA's Office of International and Tribal Affairs and the Office of Science Policy. It has been subjected to Agency review and approved for publication. Mention of trade names or commercial products does not constitute endorsement, certification, or recommendation for use.

We thank the NASA Goddard Earth Sciences Data Center for open distribution of AURA data. Some of the analyses and visualizations used in this paper were produced with the Giovanni online data system, developed and maintained by the NASA GES DISC.

REFERENCES

Aneja, V. (2001). Atmospheric Nitrogen Compounds II: Emissions, Transport, Transformation, Deposition and Assessment. Atmos.Environ. 35: 1903–1911.

Boersma, K.F., Eskes, H.J. and Brinksma, E.J. (2004). Error analyses for tropospheric NO2 retrieval from space, J. of Geophys. Res., 109, doi:10.1029/2003JD003962.

Boersma, K.F., Eskes, H.J., Veefkind, J.P., Brinksma, E.J., van der A, R.J., Sneep, M., van den Oord, G.H.J., Levelt, P.F., Stammes, P., Gleason, J.F. and Bucsela, E.J. (2007). Near-real time retrieval of tropospheric NO_2 from OMI, Atmos. Chem. Phys, 7, 2103–2118. doi:10.5194/acp-7-2103-2007

Duncan, B.N., Yoshida, Y., Olson, J.R., Sillman, S., Martin, R.V., Lamsal, L., Hu, Y., Pickering, K.E., Retscher, C., Allen, D.J. and Crawford, J.H. (2010). Application of OMI Observations to a Space-Based Indicator of NOx and VOC Controls on Surface Ozone Formation. Atmos. Environ. 44(21-22): 2625-2631.

EPA. (2006). Air Quality Criteria for Ozone and Related Photochemical Oxidants. U.S. EPA EPA 600/R-05/004aF, National Center for Environmental Assessment, Research Triangle Park, NC, USA, 2006, 821 p. Available online at: http://www.epa.gov/ncea/isa/index.htm.

Forster, P., Ramaswamy, V., Artaxo, P., Berntsen, T., Betts, R., Fahey, D., Haywood, J., Lean, J., Lowe, D., Myhre, G., Nganga, J., Prinn, R., Raga, G., Schulz, M. and van Dorland, R.

(2007). Changes in Atmospheric Constituents and in Radiative Forcing. In: S. Solomon et al. (Editors), Climate Change 2007: The Physical Science Basis. Contribution of Working Group I to the Fourth Assessment Report of the Intergovernmental Panel on Climate Change, Cambridge University Press, Cambridge, United Kingdom and New York, NY, USA.

Fuhrer, J. and Booker, F. (2003). Ecological Issues Related to Ozone: Agricultural Issues. Environ. Internat. 29: 141–154.

Guicherit, R. and Roemer, M. (2000). Tropospheric Ozone Trends. Chemosphere. – Global Change Sci. 2: 167-183.

Gurjar, B.R., Molina, L.T. and Ojha, C.S.P. (2010). Air Pollution. Health and Environmental Impacts, CRC Press, Boca Raton.

Ionov, D., Sinyakov, V. and Semenov, V. (2006). Validation of GOME (ERS-2) NO_2 vertical column data with ground-based measurements at Issyk-Kul (Kyrgyzstan), Advances in Space Research, 37, 2254–2260. doi:10.1016/j.asr.2005.11.011.

Ionov, D.V., Timofeyev, Y.M., Sinyakov, V.P., Semenov, V.K., Goutail, F., Pommereau, J.-P., Bucsela, E.J., Celarier, E.A. and Kroon, M. (2008). Ground-based validation of EOS-Aura OMI NO2 vertical column data in the midlatitude mountain ranges of Tien Shan (Kyrgyzstan) and Alps (France). J. Geophys. Res.: 113(D15).

James, I.N. (1995). Introduction to Circulating Atmospheres, 1st pbk. ed. (with corrections), Cambridge Atmospheric And Space Science Series, Cambridge University Press, Cambridge, New York.

Jonson, J.E., Simpson, D., Fagerli, H. and Solberg, S. (2006). Can We Explain the Trends in European Ozone Levels? Atmos. Chem. Phys. 6: 51–66.

Kumar, U., Prakash, A. and Jain, V.K. (2008). A Photochemical Modelling Approach to Investigate O_3 Sensitivity to NOx and VOCs in the Urban Atmosphere of Delhi, Aerosol and Air Quality Research, 8, 147–159.

Lamsal, L.N., Martin, R.V., van Donkelaar, A., Celarier, E.A., Bucsela, E.J., Boersma, K.F., Dirksen, R., Luo, C. and Wang, Y. (2010). Indirect validation of tropospheric nitrogen dioxide retrieved from the OMI satellite instrument: Insight into the seasonal variation of nitrogen oxides at northern midlatitudes, J. Geophys. Res, 115.

Levelt, P., van den Oord, G., Dobber, M., Malkki, A., Visser, H., de Vries, J., Stammes, P., Lundell, J. and Saari, H. (2006). The Ozone Monitoring Instrument, IEEE Trans. Geosci. Remote Sensing, 44: 1093–1101.

Martin, R.V. (2004). Space-based diagnosis of surface ozone sensitivity to anthropogenic emissions, Geophys. Res. Lett, 31. doi:10.1029/2004GL019416.

Mei, L., Xue, Y., de Leeuw, G., Guang, J., Wang, Y., Li, Y., Xu, H., Yang, L., Hou, T., He, X., Wu, C., Dong, J., and Chen, Z. (2011). Integration of remote sensing data and surface observations to estimate the impact of the Russian wildfires over Europe and Asia during August 2010. Biogeosciences, 8: 3771-3791. doi:10.5194/bg-8-3771-2011.

Miller-Schulze, J.P., Shafer, M., Schauer, J.J., Solomon, P.A., Lantz, J.J., Artamonova, M., Chen, B.B., Imashev, S.A., Sverdlik, L.G., Carmichael, G., and Deminter, J. (2011). Characteristics of Fine Particle Carbonaceous Aerosol at Two Remote Sites in Central Asia. Atmos. Environ. 45(38), 6955-6964.

Millet, D.B., Jacob, D.J., Turquety, S., Hudman, R.C., Wu, S., Fried, A., Walega, J., Heikes, B.G., Blake, D.R., Singh, H.B., Anderson, B.E. and Clarke, A.D. (2006). Formaldehyde

distribution over North America: Implications for satellite retrievals of formaldehyde columns and isoprene emission, J. Geophys. Res, 111. doi:10.1029/2005JD006853.

Morys, M., Mims, F.M., III, Hagerup, S., Anderson, S.E., Baker, A., Kia, J. and Walkup, T. (2001). Design, Calibration, and Performance of MICROTOPS II Handheld Ozone Monitor and Sun Photometer. J. Geophys. Res, 106: 14573–14582. doi.org/10.1029/2001JD900103.

Peirce, J.J. and Aneja, V.P. (2000). Nitric Oxide Emissions from Engineered Soil Systems. J. Envir. Engrg. 126: 225-232.

Seinfeld, J.H. and Pandis, S.N. (2006). Atmospheric Chemistry and Physics. From Air Pollution to Climate Change, 2nd. J. Wiley, Hoboken N.J.

Shepherd, T. (2007). Transport in the Middle Atmosphere. J. Meteor. Society Japan 85B: 165-191.

Tiwary, A. and Colls, J. (2010). Air pollution. Measurement, modelling and mitigation, 3rd, Routledge, London.

UNEP, UNDP, OSCE, NATO (2005): Environment and Security: Transforming risks into cooperation. Central Asia Fergana/Osh/Khujand area. Available online at: http://www.grida.no/files/publications/envsec/ferghana-report-eng.pdf.

Veefkind, J.P., Boersma, K.F., Wang, J., Kurosu, T.P., Krotkov, N., Chance, K. and Levelt, P. F. (2011). Global satellite analysis of the relation between aerosols and short-lived trace gases, Atmos. Chem. Phys, 11, 1255–1267. doi:10.5194/acp-11-1255-2011.

Ziemke, J.R., Chandra, S., Duncan, B.N., Froidevaux, L., Bhartia, P.K., Levelt, P.F. and Waters, J.W. (2006). Tropospheric Ozone Determined from Aura OMI and MLS: Evaluation of Measurements and Comparison with the Global Modeling Initiative's Chemical Transport Model. J. Geophys. Res: 111, D19303, doi:10.1029/2006JD007089.

380

381

Figure Captions

Figure 1. Kyrgyzstan with respect to Central Asia

Figure 2. Temporal variations of TCO at the Lidar site, Jun 2008-May-2009, data points - TCO per day during the mid-day hours

Figure 3. Seasonal maps of the spatial distribution of TCO-OMI (DU).

Figure 4. Monthly average values of total ozone (DU) for the northern mid-latitudes (40-45°), 1997-2005, TOMS Earth Probe.

Figure 5. Monthly average values of tropospheric column NO_2 (from Aura OMI), June 2008 - May 2009.

Figure 6. Annual map of tropospheric column NO_2 distribution (from Aura OMI), June 2008 - May 2009.

Figure 7. Annual map of HCHO distribution (from Aura OMI), June 2008 - May 2009.

Figure 8. Maps of the annual average distribution for TrCO (DU; Aura OMI/MLS) for July and December, 2008.

Figure 9. Monthly average values of ozone in TrCO (DU; Aura OMI/MLS), June 2008 - May 2009.

Figure 10. TrCO contribution to total ozone, June 2008 - May 2009.


Lake Balqash
KAZAKHSTAN
Urumchi
Almaty
Lidar-Site
Issyk-Kul
Bishkek
KYRGYZSTAN
Tien-Shan
Tashkent
Ferghana Valley
UZBEKISTAN
CHINA
TAJIKISTAN
AFGHANISTAN
PAKISTAN
40

Figure 1

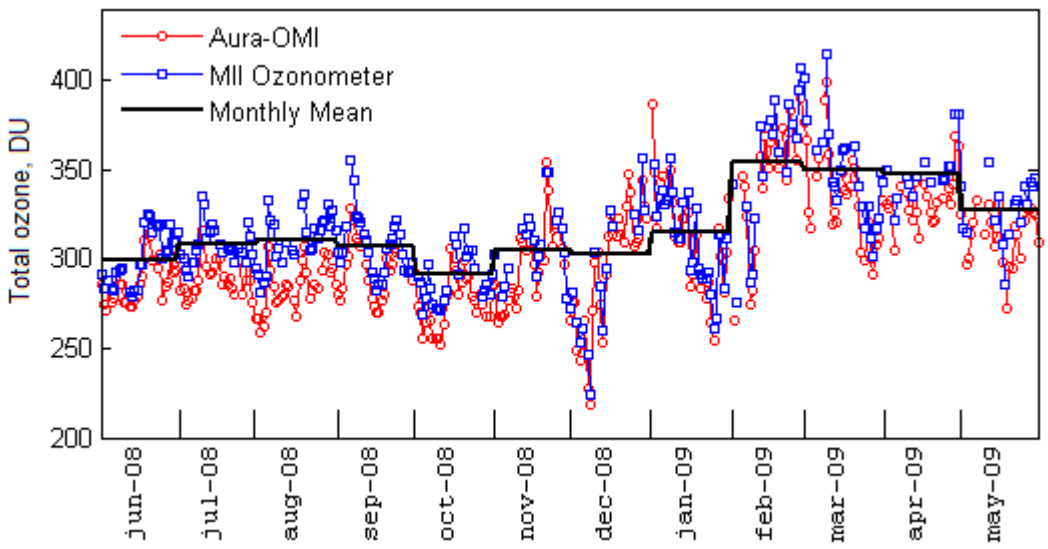
Aura-OMI
MII Ozonometer
Monthly Mean
Total ozone, DU
400
350
300
250
200
jun-08
jul-08
aug-08
sep-08
oct-08
nov-08
dec-08
jan-09
feb-09
mar-09
apr-09
may-09

Figure 2

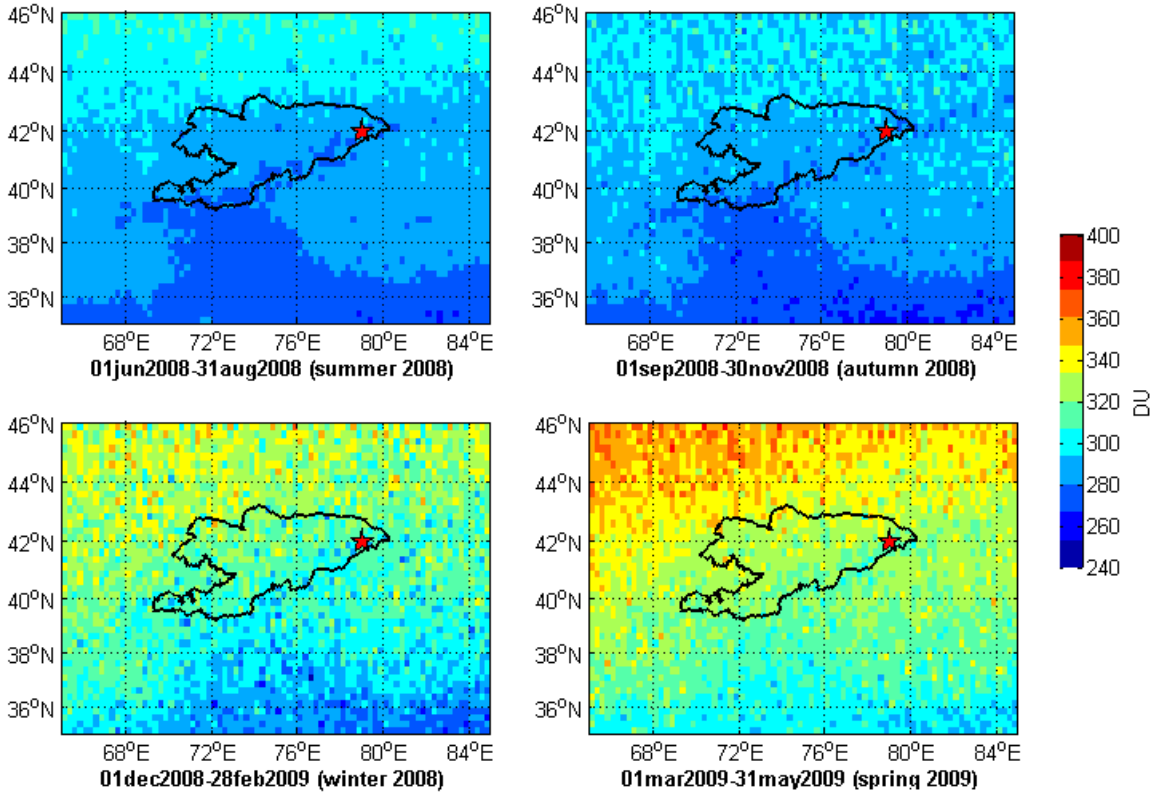
46°N
44°N
42°N
40°N
38°N
36°N
68°E
72°E
76°E
80°E
84°E
01jun2008-31aug2008 (summer 2008)
01sep2008-30nov2008 (autumn 2008)
01dec2008-28feb2009 (winter 2008)
01mar2009-31may2009 (spring 2009)
400
380
360
340
320
300
280
260
240
DU

Figure 3

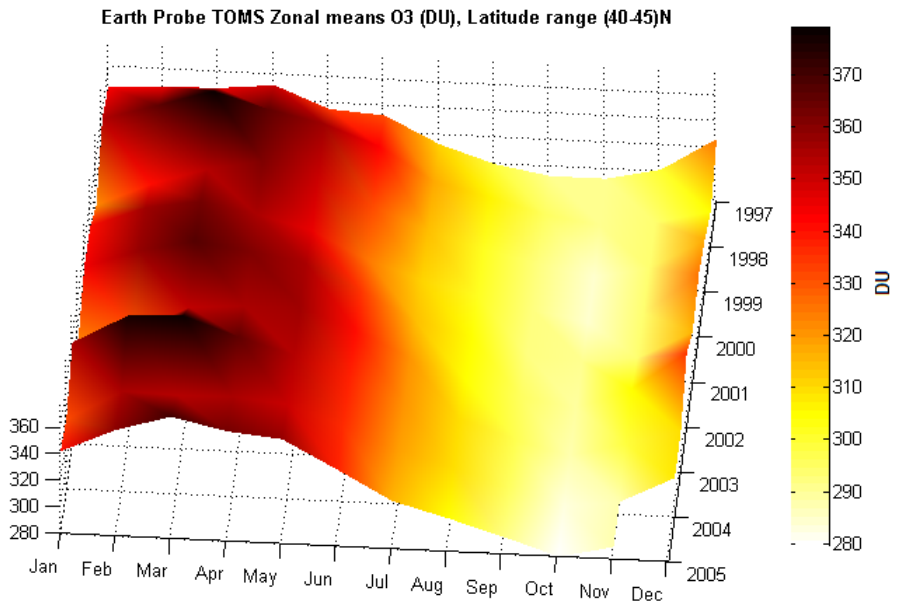
Earth Probe TOMS Zonal means O3 (DU), Latitude range (40-45)N
360
340
320
300
280
Jan
Feb
Mar
Apr
May
Jun
Jul
Aug
Sep
Oct
Nov
Dec
1997
1998
1999
2000
2001
2002
2003
2004
2005
370
360
350
340
330
320
310
300
290
280
DU

Figure 4

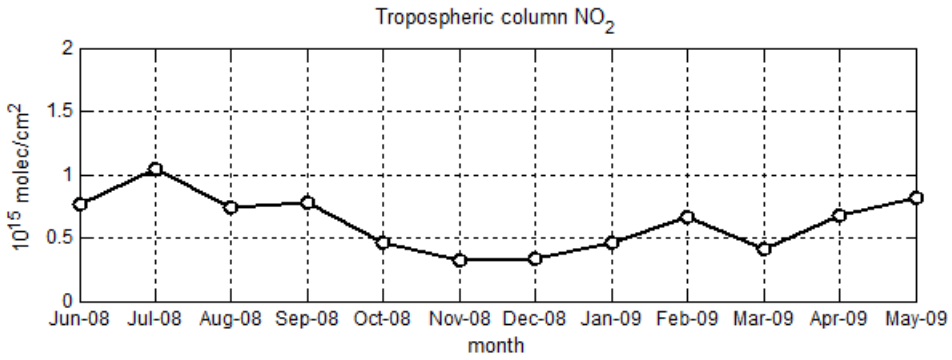
Tropospheric column NO2
10^15 molec/cm^2
2
1.5
1
0.5
0
Jun-08
Jul-08
Aug-08
Sep-08
Oct-08
Nov-08
Dec-08
Jan-09
Feb-09
Mar-09
Apr-09
May-09
month

Figure 5

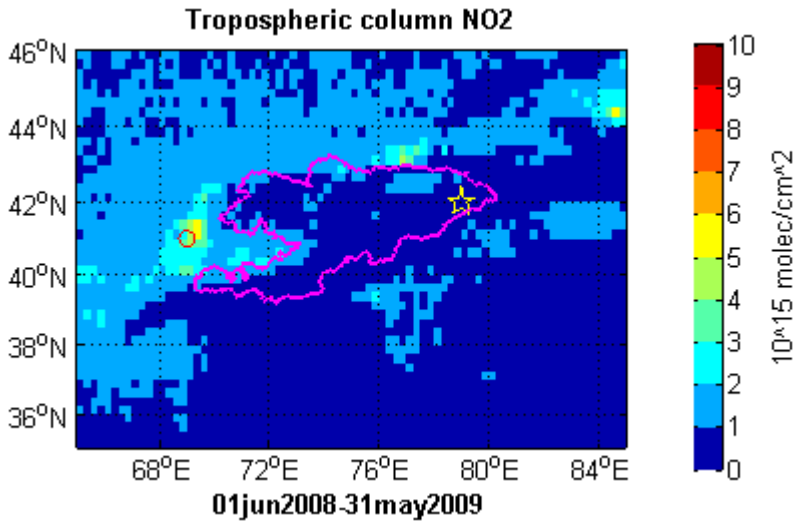
Tropospheric column NO2
46°N
44°N
42°N
40°N
38°N
36°N
68°E
72°E
76°E
80°E
84°E
01jun2008-31may2009
10
9
8
7
6
5
4
3
2
1
0
10^15 molec/cm^2

Figure 6

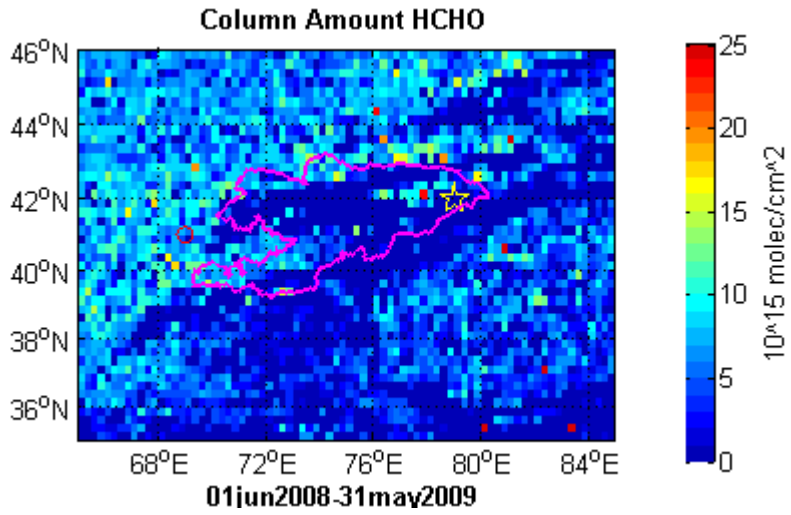
Column Amount HCHO
46°N
44°N
42°N
40°N
38°N
36°N
68°E
72°E
76°E
80°E
84°E
01jun2008-31may2009
25
20
15
10
5
0
10^15 molec/cm^2

Figure 7

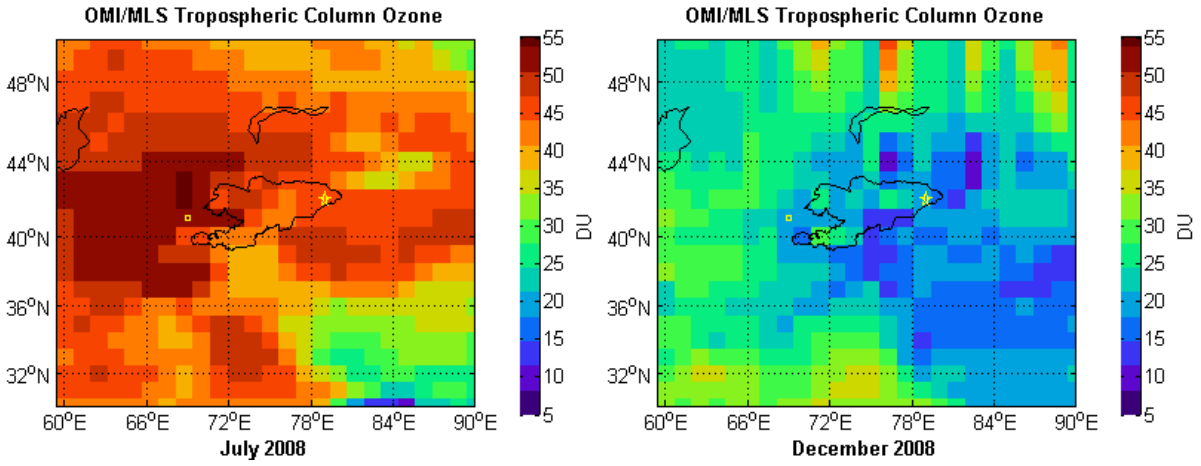
OMI/MLS Tropospheric Column Ozone
48°N
44°N
40°N
36°N
32°N
60°E
66°E
72°E
78°E
84°E
90°E
July 2008
55
50
45
40
35
30
25
20
15
10
5
DU
OMI/MLS Tropospheric Column Ozone
48°N
44°N
40°N
36°N
32°N
60°E
66°E
72°E
78°E
84°E
90°E
December 2008
55
50
45
40
35
30
25
20
15
10
5
DU

Figure 8

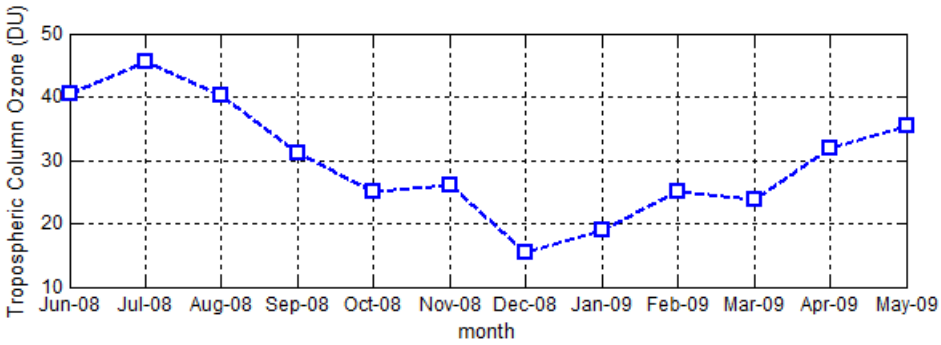
Tropospheric Column Ozone (DU)
50
40
30
20
10
Jun-08
Jul-08
Aug-08
Sep-08
Oct-08
Nov-08
Dec-08
Jan-09
Feb-09
Mar-09
Apr-09
May-09
month

Figure 9

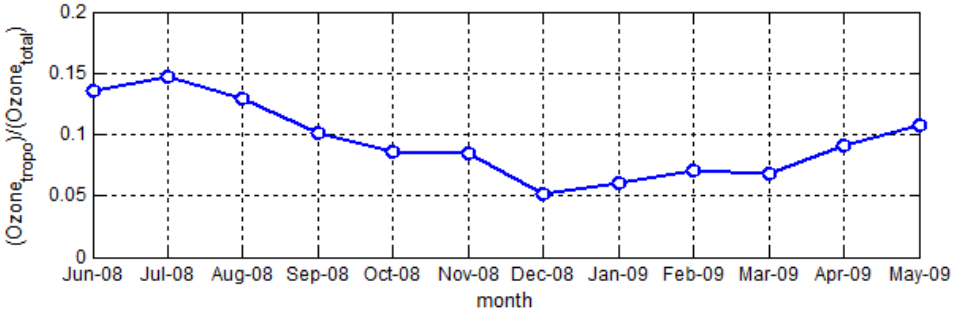
0.2
0.15
0.1
0.05
0
(Ozone_tropo)/(Ozone_total)
Jun-08
Jul-08
Aug-08
Sep-08
Oct-08
Nov-08
Dec-08
Jan-09
Feb-09
Mar-09
Apr-09
May-09
month

Figure 10